

# THE CLUSTERING OF MERGING STAR-FORMING HALOES

## Dust emission as high-frequency CMB foreground

M. Righi<sup>1</sup>, C. Hernandez-Monteagudo<sup>2</sup>, R.A. Sunyaev<sup>1,3</sup>

1 – MPA (Garching)  
2 – Univ. of Pennsylvania (Philadelphia)  
3 – IKI (Moscow)



MAX-PLANCK-GESELLSCHAFT

### ABSTRACT

Future observations of CMB anisotropies will be able to probe high multipoles of the angular power spectrum, corresponding to a resolution of a few arcminutes. Dust emission from merging galaxies is one of the foregrounds that will affect such very small scales. We estimate the contribution to CMB angular fluctuations from objects which are bright in the sub-millimeter band due to intense star formation bursts following merging episodes. We base our approach on the Lacey-Cole merger model and on the Kennicutt relation which connects the star formation rate in galaxies with their infrared luminosity. We set the free parameters of the model in order to not exceed the SCUBA source counts, the Madau plot of star formation rate in the universe and the COBE/FIRAS data on the intensity of the sub-millimeter cosmic background. We show that the angular power spectrum arising from the distribution of such star-forming haloes will be one of the most significant foregrounds in the high frequency channels of forthcoming CMB experiments, such as PLANCK, ACT and SPT. The correlation term, due to the clustering of multiple merging haloes at redshift  $z \sim 2-6$ , is dominant in the broad range of angular scales  $200 < l < 3000$ . Poisson fluctuations due to bright sub-millimeter sources are more important at higher  $l$ , but since they are generated from the brightest sources, such contribution could be strongly reduced if bright sources are excised from the sky maps. The contribution of the correlation term to the angular power spectrum depends strongly on the redshift evolution of the escape fraction of UV photons. The measurement of this signal will therefore give important information about the sub-millimeter emission and the escape fraction of UV photons from galaxies, in the early stage of their evolution.

### STAR FORMATION IN MERGING AND LUMINOSITY FUNCTION

We model the star formation within the framework of the halo model and derive the star formation rate as the rate of the baryonic mass that is accreted into new haloes. The mass of new stars created into each merging episode is proportional to the baryonic mass of the merging haloes, according to an efficiency parameter ( $\eta=5\%$ ). Only the haloes with a cooling time shorter than Hubble time are considered.

We then introduce a characteristic timescale for the star formation, following the results of numerical simulation of gas-rich merging galaxies (e.g. Springel & Hernquist 2005). We identify three phases of star formation activity (Figure 1): a long underlying phase (red), with a low and constant star formation rate, which is independent of the major merging process and it is merely the sum of the quiescent star formation rates in each disk prior to the encounter; a second, more active phase (green), which corresponds to the first close passage of one galaxy around the other, with a timescale of the order of 300 Myr; a strong starburst phase (blue), which occurs when the two galaxies finally merge together, with a very short timescale lower than 100 Myr. Only the latter two phases are connected with the merging activity and are therefore included in the model.

Once the star formation rate in each merging object is known, it is straightforward to derive the corresponding far-infrared (8-1000  $\mu\text{m}$ ) luminosity through the Kennicutt relation (Kennicutt 1998)

$$\dot{M}_* [M_\odot/\text{yr}] = 1.71 \times 10^{-10} L_{\text{FIR}} [L_\odot]$$

The bulk of the emission in the FIR band peaks around 100  $\mu\text{m}$  and is due to low temperature dust (Lagache et al. 2005). We can directly use this relation to get the luminosity due to low temperature dust in star-forming galaxies. The number density of merging objects in the universe can be derived in the context of the extended Press-Schechter formalism (Lacey & Cole, 1993) and allows us to obtain the FIR luminosity function of star-forming merging objects.

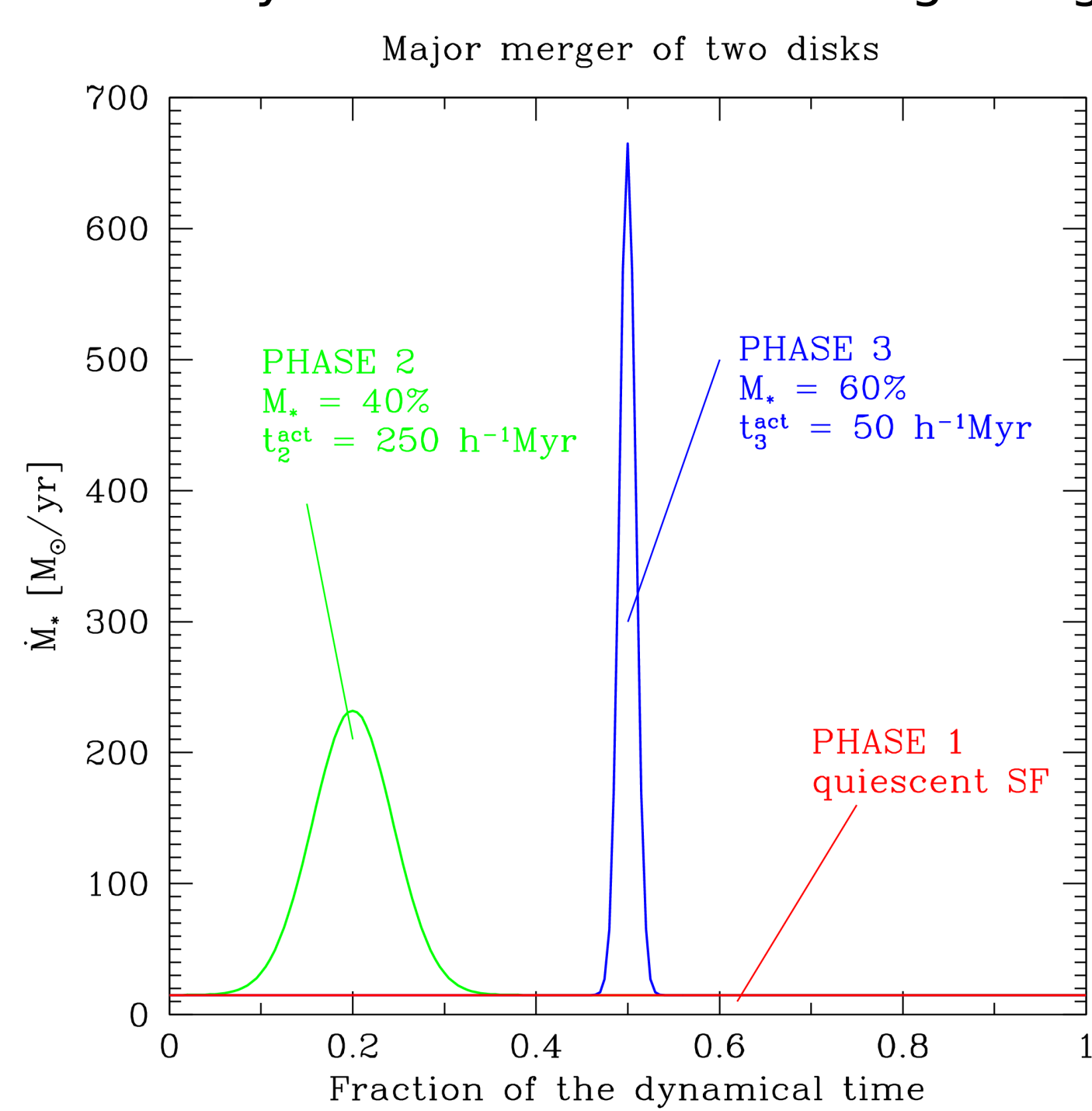


Figure 1. The star formation rate as a function of time during a merger of the gas-rich massive galaxies used for the computations in this work. Different colours identify different phases of star formation activity

### DUST EMISSION MODEL

The dust emission from galaxies in the FIR band can be well fitted by a single-temperature graybody spectrum, characterized by two spectral parameters: emissivity index  $\beta$  and dust temperature  $T_{\text{dust}}$

$$L_\nu \propto \nu^\beta B_\nu(T_{\text{dust}})$$

SCUBA observations both in the local (Dunne & Eales 2001) and in the high-redshift universe (Chapman et al. 2005) give a range  $30 < T < 50$  K for the dust temperature and  $1.0 < \beta < 2.0$  for the emissivity index. Corrections for the dust temperature evolution with redshift (Blain 1999) and for the spectral energy distribution according to the presence of the CMB thermal bath are included in the model.

### OBSERVATIONAL TESTS AND MODEL CALIBRATION

Our model depends on several free parameters which can be calibrated using three main observational tests: Madau plot for cosmic star formation history (which allows us to test the merging model), the SCUBA source number counts (to choose the best values for the spectral parameters) and the intensity of the far-infrared background according to the observation of COBE/FIRAS (to calibrate the Kennicutt relation taking into account the effect of the escape fraction of UV photons).

Figure 2 shows our prediction for the cosmic star formation history compared with a compilation of observations by Hopkins & Beacom (2006): the agreement is rather good, with a slight overestimate at  $z > 5$  which could be due to the limitation of the merging model which is known to be not very accurate at high redshift when compared to the results of N-body simulations.

The integral source counts compared with SCUBA results are displayed in Figure 3: the closest result is obtained with a value of 30 K for the dust temperature and an emissivity index  $\beta=1.5$ , in good agreement with the observations. The deficiency of sources at intermediate and low fluxes, compared with SCUBA, leads us to the conclusion that SCUBA observed objects of different nature and only 50% of them were merging galaxies. This conclusion is confirmed by the redshift distribution of the sources: SCUBA observed a peak at  $z \sim 2.5$ , while our model predicts a peak at  $z \sim 1.5$ . Future observations with the tremendous resolution and sensitivity of ALMA

will give important clues about the nature of the SCUBA sources which is still matter of discussion.

As a final test, we compute the intensity of the far-infrared background and compare with COBE/FIRAS data (Fixsen et al. 1998). To satisfy these limits we need to reduce the luminosity of the sources introducing a correction to the Kennicutt relation based on the escape fraction of UV photons. We model the escape fraction as a mass-dependent quantity, based on the assumptions that more massive objects have higher amount of dust and lower escape fraction. On the other hand, low mass objects are expected to have lower metallicity, lower dust abundances and higher escape fraction. This reduces the FIR luminosity of less massive objects and allow us to fulfill the  $1\sigma$  limit of the infrared background observed by COBE/FIRAS (Figure 4).

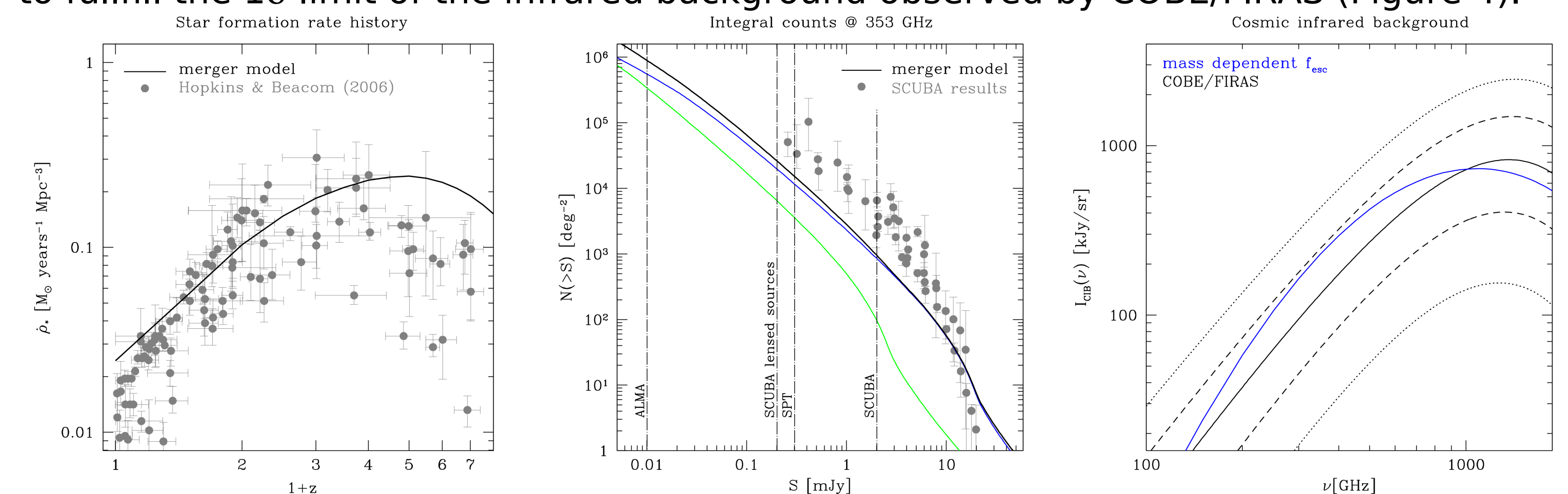


Figure 2. The cosmic SFR predicted by our model (solid line) compared with the observations (dots)

Figure 3. The integral source counts compared with SCUBA. Colours refer to the two SF phases as in Figure 1.

Figure 4. The intensity of the FIR background after the introduction of the escape fraction correction.

### RESULTS

We express the power spectrum as the sum of a Poisson plus a correlation term, which is due to the clustering of the sources. The results are presented in Figure 5: the correlation dominates up to  $l \sim 2000-4000$ , at smaller scales the Poisson is more important. However, since the Poisson power is mainly generated by the less abundant brightest sources, it will be possible to reduce it if the such sources are excised from the map, as shown in Figure 6 for the 279 GHz channel of ACT. The bulk of the correlation power comes from sources in the redshift range  $z=2-6$  (Figure 7), practically independently on the multipole index.

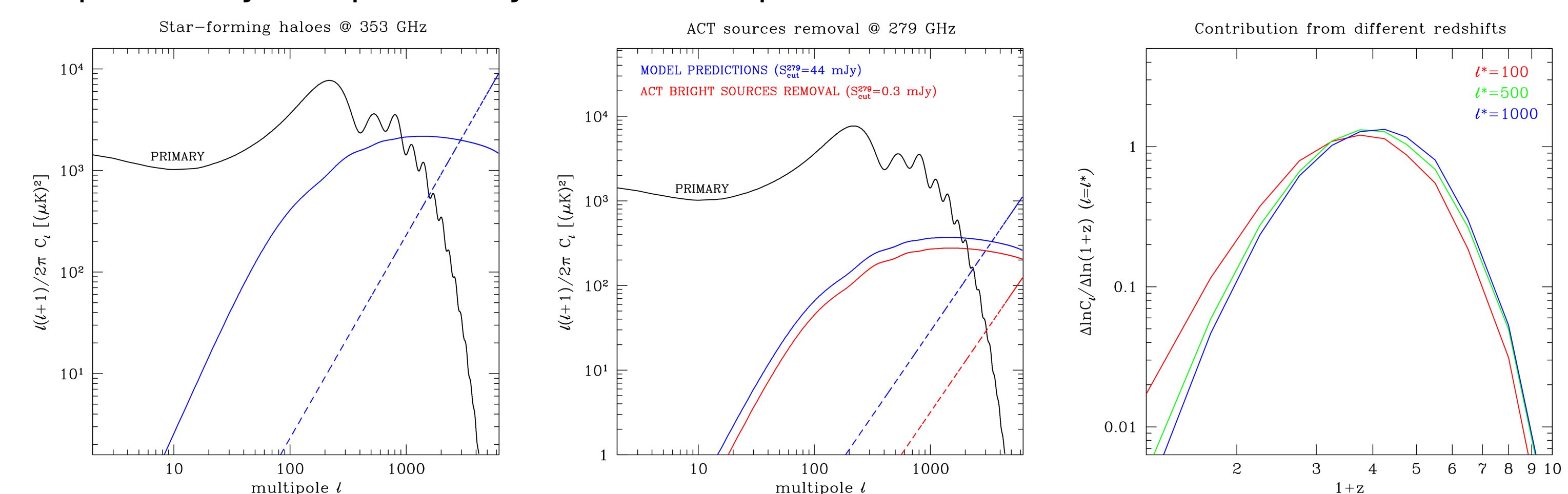


Figure 5. The power spectrum of merging star-forming haloes: correlation (solid) and Poisson (dashed).

Figure 6. The reduction of the Poisson term after the removal of brightest sources according to ACT sensitivity.

Figure 7. The contribution to the correlation term from different redshift at different multipole  $l$ .

The correlation term due to the clustering of merging star forming haloes will be one of the most important small-scale foreground sources for the high-frequency channels of the future CMB experiments (PLANCK, SPT and ACT). The predictions are in good agreement with previous estimates (Haiman & Knox 2000, Gonzalez-Nuevo et al. 2005, Toffolatti et al. 2005). If the signal will be detected, it could give important information about properties of the sources in particular about dust temperature and abundance.

### REFERENCES

- Blain, A.W. 1999, MNRAS, 309, 955
- Chapman, S.C., Blain, A.W., Smail, I., & Ivison, R.J. 2005, ApJ, 622, 772
- Dunne, L. & Eales, S.A. 2001, MNRAS, 327, 697
- Fixsen, D.J., Dwek, E., Mather, J.C., Bennett, C.L. & Shafer, R.A. 1998, ApJ, 508, 123
- Gonzalez-Nuevo, J., Toffolatti, L. & Argueso, F. 2005, ApJ, 621, 1
- Haiman, Z. & Knox, L. 2000, ApJ, 530, 124
- Hopkins, A.M. & Beacom, J.F. 2006, ApJ, 651, 142
- Kennicutt, Jr., R.C. 1998, ARA&A, 36, 189
- Lacey, C. & Cole, S. 1993, MNRAS, 262, 627
- Lagache, G., Puget, J.-L., & Dole, H. 2005, ARA&A, 43, 727
- Springel, V. & Hernquist, L. 2005, ApJ, 622, L9
- Toffolatti, L., Negrello, M., Gonzalez-Nuevo, J., et al. 2005, A&A, 613, 898

- CONTACT: righi@mpa-garching.mpg.de -